

Compact Multi-Layer Four-Way SIW Power Combiners/Dividers Operating at W-Band

Kaimin Wu, Yongjun Huang*, Hai Hu, Yao Wang, Jian Li, and Guangjun Wen

Abstract—In this paper, two compact multi-layer four-way substrate integrated waveguide (SIW) power combiners/dividers operating at W-band are analyzed and demonstrated experimentally/numerically. Based on the double-layer SIW broadside slot directional coupler, a four-way power combiner/divider is proposed for the first time. And a four-layer four-way SIW power combiner/divider is demonstrated experimentally, by using the transition structure between high-performance multi-layer SIWs and rectangular waveguide. Both SIW power combiners/dividers show high port-isolation, low loss, high efficiency, wide-band, and small lateral size.

1. INTRODUCTION

High power amplifier is an indispensable key component in the transmitter of wireless communication system [1]. With the rapid development toward higher frequency of wireless communication system, the demand for higher frequency, higher efficiency, greater bandwidth, more power capacity devices grows fast recently [2–5]. With the increasing of operating frequency, however, the size and power capacity of the solid state power devices are significantly reduced, and single solid power device is difficult to meet the requirements of a whole system. In view of this issue, the power combining technology is usually used to achieve higher power amplification in the transmitting system [6–8]. Specifically, the spatial combining technology has remarkable superiority in multi-channel power combining, since its combining efficiency is hardly affected by the combining number. Moreover, uniting the advantages of a new type of electromagnetic waveguide structure—substrate integrated waveguide (SIW) [9] and the spatial power combining technology, various power combining implementation solutions in millimeter wave band have been proposed recently [10–12].

On the other hand, the W-band of microwave part of electromagnetic spectrum ranged from 75 to 110 GHz (wavelength: 2.7–4 mm) has very important potential applications, e.g., satellite communications, millimeter-wave radar research, military radar targeting and tracking, and some other non-military applications. For the power combining techniques operating at W-band, however, only a few works have been reported and numerically/experimentally demonstrated [13–17].

In this paper, we analyze and demonstrate experimentally/numerically two kinds of compact multi-layer four-way SIW power combiners/dividers operating at W-band. Firstly, based on the double-layer SIW broadside slot directional coupler, a four-way power combiner/divider is proposed for the first time to our knowledge. Secondly, a four-layer four-way SIW power combiner/divider is demonstrated experimentally, based on the transition structure between high-performance multi-layer SIWs and rectangular waveguide. Both SIW power combiners/dividers show high port-isolation, low loss, high efficiency, wide-band, and small lateral size.

Received 23 December 2015, Accepted 28 January 2016, Scheduled 4 February 2016

* Corresponding author: Yongjun Huang (yongjunh@uestc.edu.cn).

The authors are with the Centre for RFIC and System Technology, School of Communication and Information Engineering, University of Electronic Science and Technology of China, Chengdu 611731, China.

2. FOUR-WAY POWER COMBINER/DIVIDER BASED ON THE DOUBLE-LAYER SIW BROADSIDE SLOT DIRECTIONAL COUPLER

We start by analyzing the four-way power combiner/divider based on the double-layer SIW broadside slot directional coupler. As shown in Fig. 1(a), two SIWs are placed together and two rectangular slots made on the middle layer of the two SIWs for electromagnetic energy coupling, schematically shown in Fig. 1(d). Such a directional coupler is developed from a multi-hole rectangular waveguide coupler and/or SIW [18], in which the distance between adjacent holes is reduced to zero. The whole system can be considered as two domains, the coupling and uncoupling domains. The coupling domain corresponds to the strip line part between the two rectangular slots, and the uncoupling domain is the regular SIW part. There is only TE_{10} mode in the uncoupling domain, while both TE_{10} and TEM modes exist in the coupling domain. As a result, the two modes are interfered, and the energy is exchanged in this region due to different phase velocities. Coupling rate highly depends on the overlap of the two modes.

Here we first roughly determine the width of the SIWs based on the rectangular waveguide theory and operating frequency range. Then considering the impedance matching between the coupling and uncoupling domains and the equal magnitude outputs for the coupler, we optimize key parameters of the two slots as shown in Fig. 1(b). By performing the finite element method based software (HFSS V14), the finalized structure parameters are optimized and shown in Table 1. A Rogers RT/duriod 5880 dielectric substrate is used in this paper, where the dielectric constant is 2.2 and loss tangent 0.0009. The numerical transmission and reflection properties for the four-port device are shown in Figs. 1(e) and (f). It is shown that the designed SIW directional coupler realizes equal power coupling for the through port (port 2) and coupled port (port 3) in the frequency range of 85 GHz–105 GHz, with inserting loss of $3.25 \text{ dB} \pm 0.2 \text{ dB}$. The return loss of port 1 is below 17.5 dB and the isolation between port 2 and port 3 below 15 dB in the whole simulating frequency band. From the phase-frequency curve shown in Fig. 1(f), the through port and coupled port keep 90 deg phase difference in the whole W-band. Therefore, such a SIW directional coupler indicates high-performance power dividing properties and can be used for our next analyzed four-way power divider.

Then, we design a four-way power divider, as shown in Fig. 2(a), by using three double-layer SIW directional couplers proposed before. The electromagnetic wave transmits from port P1 and divides

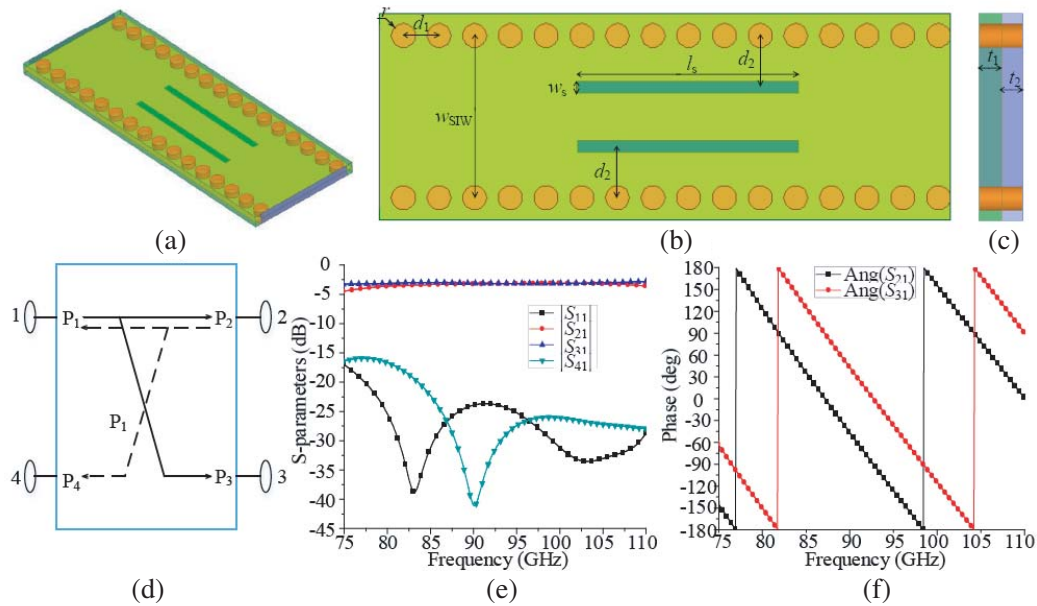


Figure 1. Double-layer SIW broadside slot directional coupler. (a) 3-D view of the coupler, (b) top view of the coupler with parameter definitions, (c) side view of the coupler shown the substrate thicknesses, (d) the schematic representation of the directional coupler, (e) the simulated magnitude of the S -parameters, and (f) the simulated phase of the transmissions.

Table 1. The optimized structural parameters of the double-layer SIW directional coupler.

d_1	d_2	l_s	r	t_1	t_2	w_{SIW}	w_s
0.35 mm	0.65 mm	2.78 mm	0.15 mm	0.127 mm	0.127 mm	2.05 mm	0.25 mm

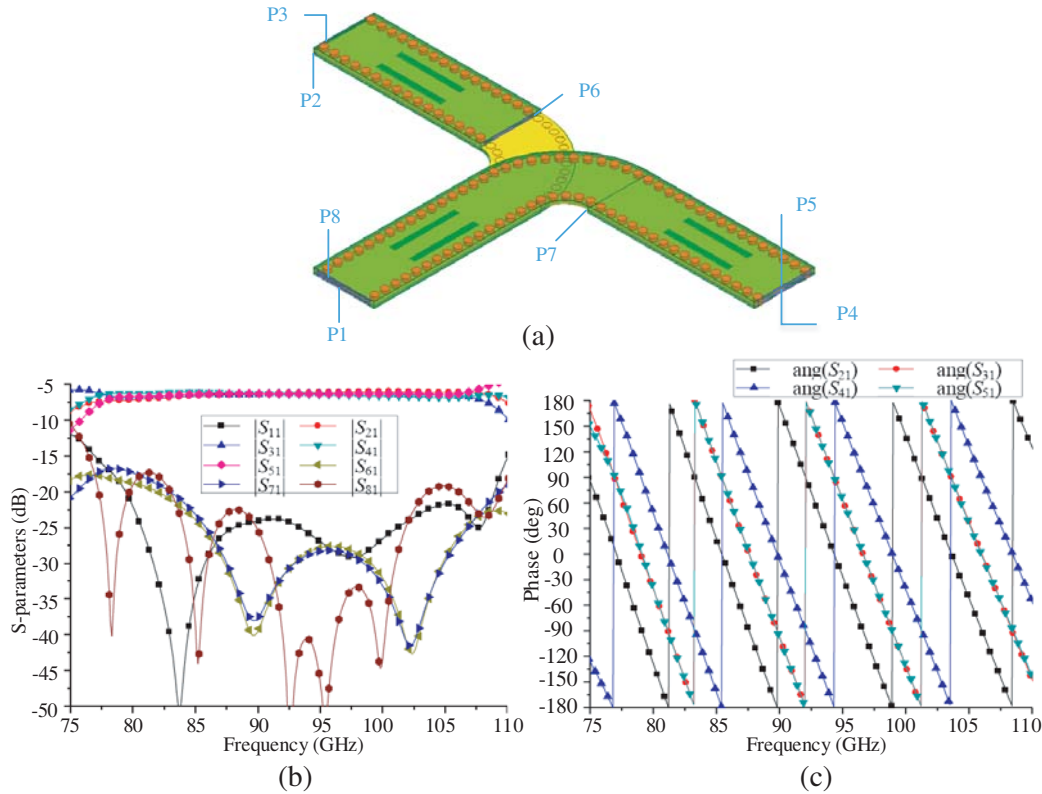


Figure 2. Four-way power divider based on the double-layer SIW directional coupler. (a) 3-D view of the divider, (b) the simulated magnitude of the S -parameters, and (c) the simulated phase properties of the designed divider.

to two equal paths at the first 3-dB coupler with 90 deg phase difference. Then the through port and coupled port of the first 3-dB coupler connect to the second and third 3-dB couplers as shown in Fig. 2(a) to keep the whole device compactly. The structural parameters of the four-way power divider are the same as shown in Fig. 1 and can be found at Table 1. The only difference is the 90 deg bent SIW part for separating the two paths. The whole optimized S -parameters performances of the device can be found in Figs. 2(b) and (c), which show that all of the four output ports (P2 to P5) have almost equal magnitude ($6.25 \text{ dB} \pm 0.3 \text{ dB}$), and all the other isolation ports indicate magnitudes below 20 dB in the W-band. Moreover, as shown in Fig. 2(c), for each output port there is a 90 deg phase difference.

To check the performance of the four-way power combiner/divider based on the double-layer SIW broadside slot directional coupler, we further connect another four-way combiner to the divider as a back-to-back combiner/divider configuration as shown in Fig. 3(a). It is very important that the phases of the four outputs of divider (see Fig. 2(a)) are quite different so we need carefully design and connect the back-to-back combiner to match the phase differences. As shown in Fig. 3(a), the centrosymmetry configuration can satisfy the phase condition, so the output of the combiner (P2) can get the maximum power. It can be confirmed from the simulated electrical field distributions in the combiner/divider as shown in Fig. 3(c). Specifically, only the two ports (P1 and P2) on the bottom SIW layer show complete electrical field path, and there is no power leakage at ports P8 and P3.

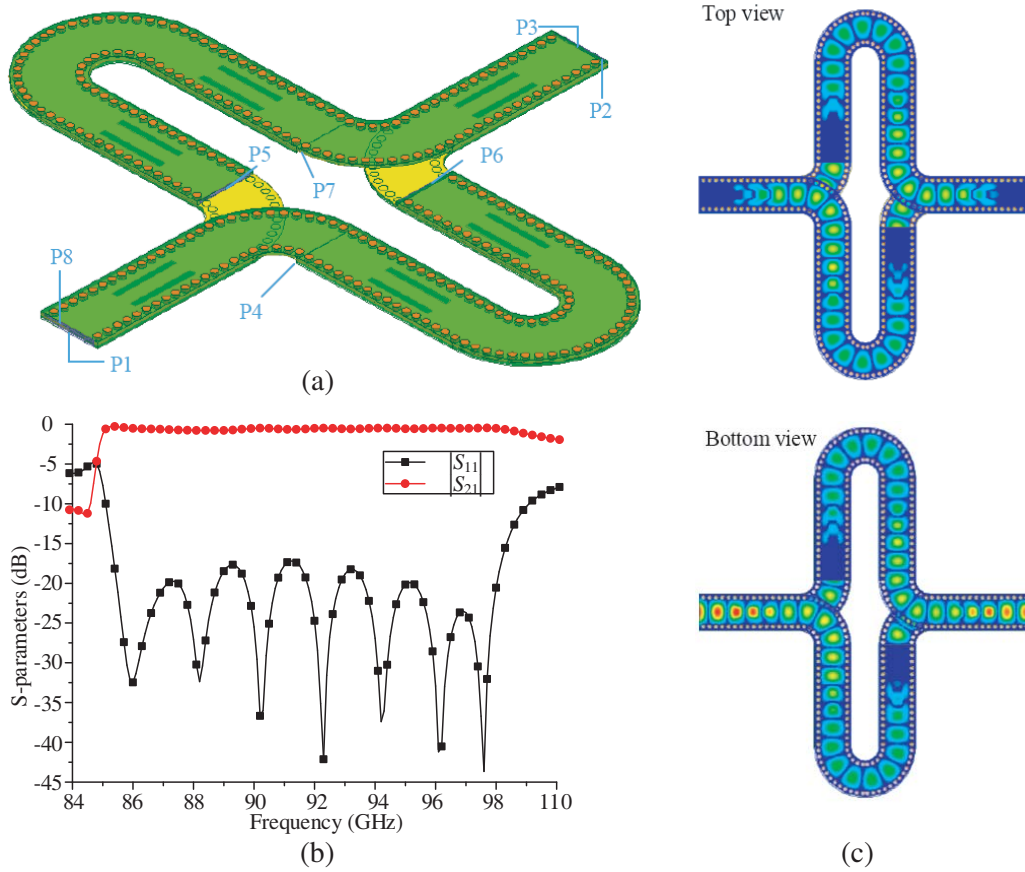


Figure 3. The back-to-back power divider/combiner based on the double-layer SIW broadside slot directional coupler. (a) 3-D view of the divider/combiner, (b) the simulated magnitude of the transmission and reflection, and (c) the simulated electrical field distributions for the power divider/combiner.

From the simulated transmission and reflection properties for the whole four-way power combiner/divider, the inserting loss is $0.6 \text{ dB} \pm 0.2 \text{ dB}$, and the return loss is larger than 17.5 dB in the frequency range of 85 GHz to 98 GHz. It means that the power combining efficiency can reach about 93%.

3. FOUR-WAY POWER COMBINER/DIVIDER BASED ON THE TRANSITION STRUCTURE BETWEEN MULTI-LAYER SIWS AND RECTANGULAR WAVEGUIDE

To experimentally measure the real transmission/reflection properties of the above discussed four-way power combiner/divider, two rectangular waveguide to SIW transitions are needed. However, it is well known that the rectangular waveguide and SIW possess the same propagation mode (TE_{10}), so it is already a good transition configuration. Moreover, rectangular waveguide can be used to the main transmission component in the power amplifier application due to its high power capacity. Therefore, in this section we design a four-way power combiner/divider by directly using the transition structure between multi-layer SIWs and rectangular waveguide.

Firstly, the multi-layer SIWs to rectangular waveguide transition structure (actually also the four-way power divider) are analyzed and designed as shown in Fig. 4(a). Generally, the heights of the rectangular waveguide and four-layer SIWs are different. Therefore, we need insert a height-reduced or

height-enhanced waveguide transition between the regular rectangular waveguide and four-layer SIWs. Moreover, the dielectric parameters between the rectangular waveguide and SIWs are quite different, so we need some more transition techniques as well to prevent the electromagnetic wave reflection due to the mode and impedance mismatches. In this section, a 0.254 mm Rogers RT/duriod 5880 dielectric substrate is used to the four-layer SIWs. The copper cladding of the substrate is 0.017 mm, and the height of the WR10 regular rectangular wave is 1.27 mm. As shown in Fig. 4(a), the height-reduced waveguide (reduction is 0.169 mm) and the prism-shaped and gradient-shaped dielectrics are used in this transition structure between multi-layer SIWs and rectangular waveguide. Based on the chosen dielectric substrate, the key structural parameters shown in Fig. 4(b) are optimized by HFSS and concluded in Table 2.

Based on the above optimized structural parameters, the simulated S -parameters of the four-way power divider based on the transition structure between multi-layer SIWs and rectangular waveguide (see Fig. 4(a)) are shown in Figs. 4(c) and (d). It can be seen that four output ports have almost the

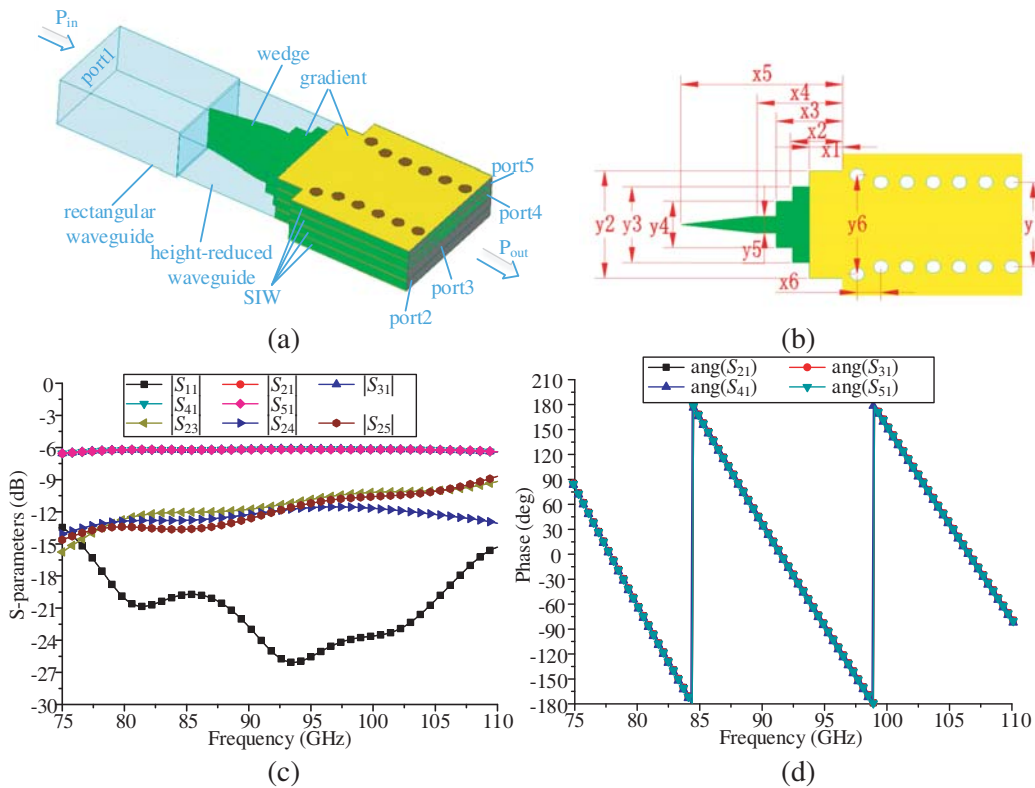


Figure 4. Four-way power divider based on the transition structure between multi-layer SIWs and rectangular waveguide. (a) 3-D view of the divider, (b) the top view shown the structural parameters definitions, (c) the simulated magnitude of the S -parameters, and (d) the simulated phase properties of the designed divider.

Table 2. The concluded structural parameters of the multi-layer SIWs to rectangular waveguide transition.

x_1	x_2	x_3	x_4	x_5	x_5
0.7 mm	1.1 mm	1.4 mm	1.8 mm	3.4 mm	0.5 mm
y_1	y_2	y_3	y_4	y_5	y_5
2 mm	2.54 mm	1.8 mm	1.1 mm	0.4 mm	2.36 mm

same power level in the whole W-band ($6.3 \text{ dB} \pm 0.15 \text{ dB}$), and the port isolations among the four output ports are below 10 dB. The phases of all the four output ports are almost the same.

Next, by using the above obtained four-way power divider based on the multi-layer SIWs to rectangular waveguide transition, we design and fabricate a real four-way power combiner/divider. We use a similar back-to-back combiner/divider configuration (see Fig. 3(a)) to realize the new four-way power combiner/divider. At the same time, considering the future application (spatial power amplification), the amplifiers should be soldered somewhere in the power combiner/divider. The interaction among the four paths and the heat radiations should be taken into account as well. Therefore, the four-way SIWs are separated to two branches, and additional microstrip lines are inserted within the SIWs for the space used to solder amplifiers. The finalized four-way power combiner/divider is designed and shown in Fig. 5(a). It can be seen that there is no more transition between SIW and microstrip line because the length of microstrip line is small (4 mm), and the electromagnetic energy can be transmitted in this region properly.

Based on this design and the optimized structural parameter shown in Table 2, the simulated transmission and reflection of the four-way power combiner/divider are shown in Fig. 5(b). The results

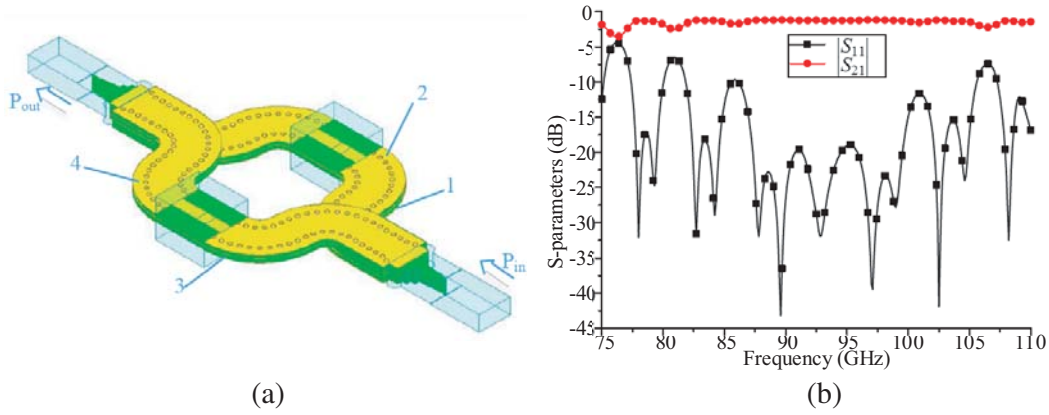


Figure 5. Four-way back-to-back power combiner/divider based on the transition structure between multi-layer SIWs and rectangular waveguide. (a) 3-D view of the combiner/divider, (b) the simulated magnitude of the transmission and reflection.

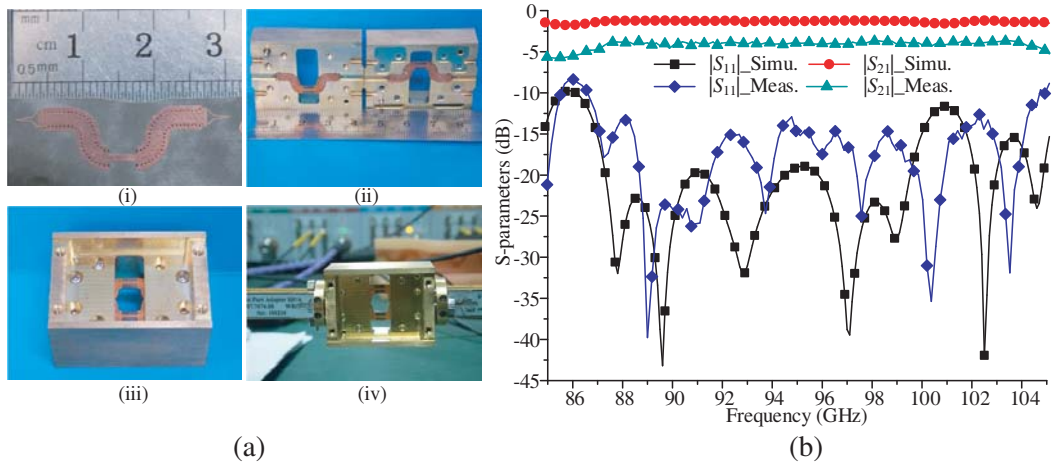


Figure 6. The fabricated four-way power combiner/divider based on the transition structure between multi-layer SIWs and rectangular waveguide. (a) The fabricated sample and measurement setup, and (b) the measured transmission and reflection.

show that the inserting loss is about $1.25 \text{ dB} \pm 0.1 \text{ dB}$, and return loss is larger than 20 dB in the frequency range of 87.5 GHz–99.5 GHz. Bad performances are found in the lower and higher frequency regions of the whole simulating frequency band. This issue can be solved by further optimizing the whole structural parameters, including microstrip line part and transition part between multi-layer SIWs and rectangular waveguide.

Finally, we fabricate the designed four-way power combiner/divider based on the multi-layer SIWs to rectangular waveguide transition. To get the real four-way power combiner/divider, the four-layer SIWs are fabricated layer-by-layer through standard printed circuit board technique on the 0.254 mm Rogers RT/duriod 5880 dielectric substrate with cooper thickness of 0.017 mm. One fabricated single-layer SIW can be found in Fig. 6(a-i). Then the four SIW layers are combined and fixed tightly by using the fabricated metallic rectangular waveguide with flanges as shown in Figs. 6(a-ii) and (a-iii). Lastly, the assembled four-way power combiner/divider is connected to an R&S ZVA67 vector network analyzer (see Fig. 6(a-iv)) with frequency converters which can cover the whole W-band. The thru-reflect-line (TRL) calibration procedure is performed to eliminate the system errors during measurements.

The measured transmission and reflection properties of the power combiner/divider are shown in Fig. 6(b), and the the corresponding numerical results are represented as well for comparisons. It is seen that the measured inserting loss is $3.9 \text{ dB} \pm 0.45 \text{ dB}$, and return loss is larger than 12 dB in the frequency range of 88.5 GHz–101 GHz, which means that the measured performance is worse than the corresponding numerical results. This mainly comes from several reasons: (1) fabrication tolerance, (b) assembling process, and (3) measurement process. The first problem can be solved by using higher quality fabrication process such as lithography technique, and the last two problems can be further reduced by carefully performing the experiments and calibrations. The overall performance of the power combiner/divider, however, remains well which shows a combining efficiency of about 63.8%.

Here we compare the key performances between our designs and some other reported methods as shown in Table 3. It is shown that our designs can achieve comparable performances for the previous reported designs. And the above designed two W-band four-way power combiners/dividers show high port-isolation, low loss, high efficiency, wide-band, and small lateral size.

Table 3. The comparisons of various power combiners/dividers methods and performances. (RW: rectangular waveguide, MS: microstrip, RL: return loss, IL: inserting loss.).

Ref.	f (GHz)	achieved method	performance (dB)	paths
[19]	82–99	SIW T-junction	$RL < 15$	2
[16]	91–95	SIW T-junction	$RL < 15,$ $-4 < IL < -3,$	2
[13]	80–90	short-wall coupling of RW	$RL < 22,$ $-4 < IL < -3,$	2
[14]	90–100	RW circulator coupling and RW-MS transition	$RL < 20,$ $IL < -0.3$	4
[17]	92–96	RW magnetic-T and RW-MS transition	$RL < 15,$ $IL < 4$	2
design 1	85–98	wide-wall coupling of SIW	$RL < 17.5,$ $IL < 0.4$	4
design 2	88.5–99.5	multi-layer SIW-RW transition	$RL < 12,$ $IL < 3.5$	4

4. CONCLUSION

In this paper, we have proposed and demonstrated experimentally/numerically two high-performance W-band four-way power combiners/dividers based on a double-layer SIW broadside slot directional coupler and four-layer SIWs to rectangular waveguide transition, respectively. Both SIW power combiners/dividers show high port-isolation, low loss, high efficiency, wide-band, and small lateral size. These designs can be easily used in future for spatial power amplifier applications.

ACKNOWLEDGMENT

This work was supported in part by the National Natural Science Foundation of China (Grant No. 61371047) and by Research Fund for the Doctoral Program of Higher Education of China (Grant No. 20110185110014). Y. Huang also gratefully acknowledges the Scholarship Award for Excellent Doctoral Student granted by Ministry of Education of China (Grant No. A03003023901006).

REFERENCES

1. Cripps, S. C., *RF Power Amplifiers for Wireless Communications*, Artech House, 1999.
2. Hanington, G., P. F. Chen, P. M. Asbeck, and L. E. Larson, "High-efficiency power amplifier using dynamic power-supply voltage for CDMA applications," *IEEE Transactions on Microwave Theory and Techniques*, Vol. 47, No. 8, 1471–1476, 1999.
3. Sun, G. and R. H. Jansen, "Broadband Doherty power amplifier via real frequency technique," *IEEE Transactions on Microwave Theory and Techniques*, Vol. 60, No. 1, 99–111, 2012.
4. Kartikeyan, M. V., E. Borie, and M. Thumm, *Gyrotrons: High-power Microwave and Millimeter Wave Technology*, Springer Science and Business Media, 2013.
5. Agah, A., H. Dabag, B. Hanafi, P. Asbeck, L. Larson, and J. Buckwalter, "A 34% PAE, 18.6 dBm 42–45 GHz stacked power amplifier in 45 nm SOI CMOS," *2012 IEEE Radio Frequency Integrated Circuits Symposium (RFIC)*, 57–60, 2012.
6. Abbosh, A. M., "A compact UWB three-way power divider," *IEEE Microwave and Wireless Components Letters*, Vol. 17, No. 8, 598–600, 2007.
7. Song, K., F. Zhang, S. Hu, and Y. Fan, "Ku-band 200-W pulsed power amplifier based on waveguide spatially power-combining technique for industrial applications," *IEEE Transactions on Industrial Electronics*, Vol. 61, No. 8, 4274–4280, 2014.
8. Ding, J., Q. Wang, Y. Zhang, L. Wu, and X. Sun, "High-efficiency millimetre-wave spatial power combining structure," *Electronics Letters*, Vol. 51, No. 5, 397–399, 2015.
9. Wu, K., "Integration and interconnect techniques of planar and non-planar structures for microwave and millimeter-wave circuits — Current status and future trend," *2001 IEEE In Asia-Pacific Microwave Conference*, 411–416, 2003.
10. Song, K., F. Zhang, F. Chen, and Y. Fan, "Wideband millimetre-wave four-way spatial power combiner based on multilayer SIW," *Journal of Electromagnetic Waves and Applications*, Vol. 27, No. 13, 1715–1719, 2013.
11. Song, K., G. Li, Q. Duan, S. Hu, and Y. Fan, "Millimeter-wave waveguide-based out-of-phase power divider/combiner using microstrip antenna," *AEU-International Journal of Electronics and Communications*, Vol. 68, No. 12, 1234–1238, 2014.
12. Dong, J., Y. Liu, Z. Yang, H. Peng, and T. Yang, "Broadband millimeter-wave power combiner using compact siw to waveguide transition," *IEEE Microwave and Wireless Components Letters*, Vol. 25, No. 9, 567–569, 2015.
13. Zheng, P., P. Zhou, W. H. Yu, H. J. Sun, X. Lv, and H. Deng, "W-band power divider based on H-plane slot waveguide bridge," *2012 International Conference on Microwave and Millimeter Wave Technology (ICMMT)*, Vol. 2, 1–4, 2012.

14. Zhao, X., X. Q. Xie, L. Zhou, and Y. L. Wu, "Four-way power divider/combiner based on waveguide microstrip structure in W-band," *2012 International Conference on Microwave and Millimeter Wave Technology (ICMMT)*, Vol. 2, 1–4, 2012.
15. Li, C., L. B. Lok, A. Khalid, V. Papageorgiou, J. Grant, and D. R. S. Cumming, "A coplanar ring power divider with high isolation for V-band and W-band applications," *Proceedings of the 42nd European Microwave Conference*, 57–60, 2012.
16. Ma, R., M. Luo, H. Sun., Z. Li, and P. Zheng, "Design and simulation of a W-band two-way power divider based on substrate integrated waveguide," *2013 IEEE International Conference on Microwave Technology and Computational Electromagnetics (ICMTCE)*, 100–102, 2013.
17. Li, J, Y. Chu, and J. Xu, "A novel W-band solid-state power divider/combiner network based on waveguide microstrip structure," *2014 IEEE International Conference on Communication Problem-Solving (ICCP)*, 266–268, 2014.
18. Karimabadi, S. S. and A. R. Attari, "X-band multi-hole directional coupler with folded substrate-integrated waveguide," *Electromagnetics*, Vol. 35, No. 6, 404–414, 2015.
19. Chen, K., B. Yan, and R. Xu, "A novel W-band ultra-wideband substrate integrated waveguide (SIW) T-junction power divider," *2010 Proceedings of International Symposium on Signals, Systems and Electronics (ISSSE)*, 1–3, 2010.